Vertical viewing angle enhancement for the 360 degree integral-floating display using an anamorphic optic system

Munkh-Uchral Erdenebat,[1] Ki-Chul Kwon,[1] Kwan-Hee Yoo,[2] Ganbat Baasantseren,[3] Jae-Hyeung Park,[4] Eun-Soo Kim,[5] and Nam Kim[1,*]

[1]*School of Information and Communication Engineering, Chungbuk National University, Naesudong-ro 52, Heungdeok-gu, Cheongju-si, Chungbuk 361-763, South Korea*

[2]*Department of Digital Informatics and Convergence, Chungbuk National University, Naesudong-ro 52, Heungdeok-gu, Cheongju-si, Chungbuk 361-763, South Korea*

[3]*School of Information Technology, National University of Mongolia, Ikh Surguuliin gudamj 3, Sukhbaatar duureg, Ulaanbaatar 210646, Mongolia*

[4]*School of Information and Communication Engineering, Inha University, Inha-ro 100, Nam-gu, Incheon 402-751, South Korea*

[5]*HoloDigilog Human Media Research Center (HoloDigilog), 3D Display Research Center (3DRC), Kwangwoon University, Kwangwoon-ro 20, Nowon-gu, Seoul 139-701, South Korea*

**Corresponding author: namkim@chungbuk.ac.kr*

Received January 30, 2014; accepted March 10, 2014;
posted March 11, 2014 (Doc. ID 205579); published April 8, 2014

We propose a 360 degree integral-floating display with an enhanced vertical viewing angle. The system projects two-dimensional elemental image arrays via a high-speed digital micromirror device projector and reconstructs them into 3D perspectives with a lens array. Double floating lenses relate initial 3D perspectives to the center of a vertically curved convex mirror. The anamorphic optic system tailors the initial 3D perspectives horizontally and vertically disperse light rays more widely. By the proposed method, the entire 3D image provides both monocular and binocular depth cues, a full-parallax demonstration with high-angular ray density and an enhanced vertical viewing angle.

OCIS codes: (100.6890) Three-dimensional image processing; (100.3010) Image reconstruction techniques; (120.2040) Displays.
http://dx.doi.org/10.1364/OL.39.002326

Integral imaging (II) is a notable three-dimensional (3D) display technique that consists of both pickup and display. A two-dimensional (2D) elemental image array (EIA) that contains different perspectives with different depth information in each, captured through a lens array from the 3D object, is generated during the pickup process. In the display part, the EIA is reconstructed as a natural 3D image via the lens array. Displayed 3D images are provided with full-parallax and continuous-viewing features; however, limited viewing angle and depth range are the main drawbacks of the system [1–3].

The integral-floating display (IFD) using double floating lenses is a solution to the narrow depth range of the II technique [4]. Both lateral and longitudinal depth values are improved, as well, and barrel distortion is reduced compared with the use of a single floating lens [5].

Various research projects have been conducted in order to improve the viewing angle of the II display [6–12]. For example, several methods that use mechanical shifting of the lens array [6], double display devices with time multiplexing [7], a curved lens array and curved screen [8], a multiple-axis telecentric relay system [9], a negative index plano–concave lens array [10], double elemental image masks [11], and a directional projection [12] were proposed recently. But those methods did not provide a viewing angle wide enough for a comfortable viewing.

A recently reported volumetric light-field display demonstrated a 3D image in 360 degree viewing zone [13]. A 360 degree viewing zone is the biggest advantage of the light field display; however, the displayed image is provided in horizontal parallax only, where a tracking system is required in vertical parallax. Due to the achievement of only a binocular depth cue, the extremely high-speed projection is required at angular light-ray sampling in order to correctly display 3D images.

Conventional 360 degree IFD, which is a combination of IFD and light field display, was a distinguished solution to the limited viewing angle of II [14]. Here, full-parallax 3D images were successfully demonstrated with a 360 degree horizontal viewing angle in the optical experiment; however, the vertical viewing angle (VVA) was too small, only 4–6 degree, due to a function of the double floating lenses. Methods that are similar have been proposed recently, but narrow VVA remains as a problem [15,16].

In this Letter, we report a new method to enhance the VVA of 360 degree IFD by using an anamorphic optic system (AOS). With the proposed method, the VVA of system is significantly increased, compared to the conventional 360 degree IFD, and other features, such as full-parallax illumination, high angular light ray sampling, and 360 degree horizontal viewing angle is still supported.

The main structure of the proposed system is almost the same as conventional 360 degree IFD, as follows: a digital micromirror device (DMD) projector displays 2D EIAs sequentially in their generated order, then a lens array reconstructs them as 3D perspectives. Floating lenses relay the initial 3D perspectives to the center of a mirror screen where the motor rotates in synchronization, as shown in Fig. 1(a). The proposed method uses an AOS, such as a vertically curved convex mirror instead of

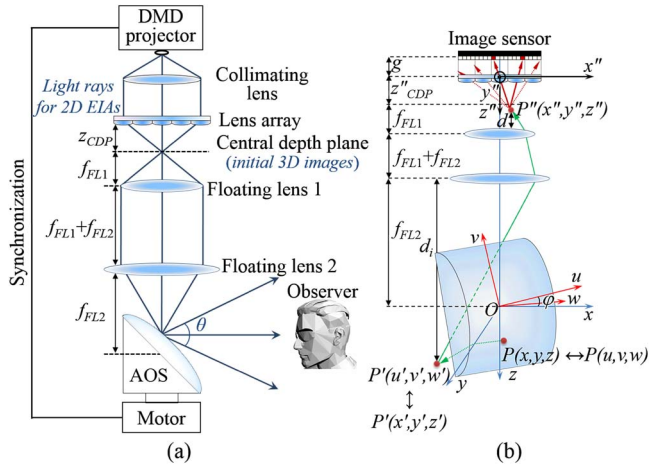

Fig. 1. (a) Schematic configuration of the proposed method and (b) EIA calculation steps for each 3D object point in the AOS space.

a typical flat mirror, to improve the VVA. The AOS disperses reflected light rays more widely in the vertical direction than a typical flat mirror, so the VVA can be expanded quite well.

EIA calculation and generation steps are shown in Fig. 1(b). EIAs are calculated for each point on the 3D object, and the generated EIA includes all of the system information. The proposed system has three coordinate systems: the main fixed world coordinates with (x, y, z) axes; local coordinates of the AOS with (u, v, w) axes, for which the origin is the same as (x, y, z) at the center of the convex mirror screen; and (x'', y'', z'') coordinates of the lens array system, for which the origin is at the center of the lens array. For a desired 3D object point P, which is illustrated in Fig. 1(b), the corresponding (u, v, w) coordinates can be determined as:

$$[u, v, w] = \left[\begin{array}{c} x\cos\varphi + y\cos(90^\circ + \varphi), \\ -\frac{x\sin\varphi + y\cos\varphi + z}{\sqrt{2}}, \frac{x\sin\varphi + y\cos\varphi - z}{\sqrt{2}} \end{array} \right] \quad (1)$$

for easier calculation of reflected points on the convex mirror, where φ is the azimuthal angle of the mirror rotation. As shown in Fig. 2, the coordinates of the reflected P' point for the corresponding object point P through the AOS is calculated with

$$[u', v', w'] = \left[u, \frac{f_m v w}{(f_m - w)^2}, \frac{f_m w}{f_m - w} \right], \quad (2)$$

where f_m is the focal length of the convex mirror. Here, coordinate values in the horizontal direction are the same as coordinates of the object point, i.e., $u' = u$, varied only in the vertical direction due to the shape of the convex mirror. In other words, the height of the displayed 3D image in the AOS space is reduced as $v/v' = w/(-w')$ proportion.

To display the correct 3D image, corresponding relayed 3D images through double floating lenses should be extended as above proportion, as shown in Fig. 2.

According to Eq. (2), improvement of the VVA can be defined as:

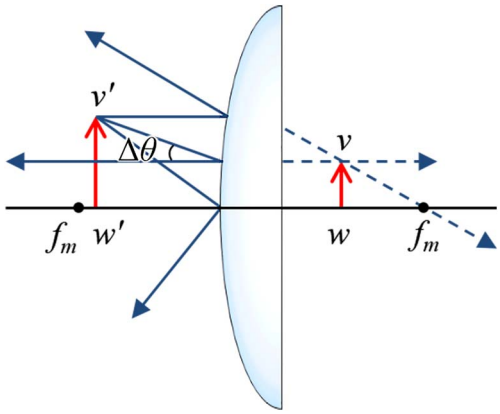

Fig. 2. Calculation of the reflected representation from the corresponding 3D object point through the AOS.

$$\Delta\theta = \arctan\left(\frac{f_m v_{\max} w_{v_{\max}} - v_{\max}(f_m - w_{v_{\max}})^2}{f_m w_{v_{\max}}(f_m - w_{v_{\max}})} \right), \quad (3)$$

where $v_{\max}$ is maximum value of v and $w_{v_{\max}}$ is the corresponding w value. From here, the f_m is the most influential parameter for VVA enhancement. Then, the mirror reflection P' is represented with (x, y, z) values as

$$[x', y', z'] = \left[\begin{array}{c} \frac{\sqrt{2}u'\cos\varphi - v'\sin\varphi - w'\sin\varphi}{\sqrt{2}}, \\ \frac{\sqrt{2}u'\cos(90^\circ + \varphi) - v'\cos\varphi - w'\cos\varphi}{\sqrt{2}}, \frac{w' - v'}{\sqrt{2}} \end{array} \right]. \quad (4)$$

The coordinates of initial 3D point P'', which is relayed through the double floating lenses from the corresponding point P', are calculated with

$$[x'', y'', z''] = \left[\frac{x' f_{\mathrm{FL1}}}{f_{\mathrm{FL2}}}, \frac{y' f_{\mathrm{FL1}}}{f_{\mathrm{FL2}}}, \frac{g f_{\mathrm{LA}} + z' f_{\mathrm{FL1}}^2}{g - f_{\mathrm{LA}} + f_{\mathrm{FL2}}^2} \right], \quad (5)$$

where f_{FL1} and f_{FL2} are the focal lengths of floating lenses, f_{LA} is the focal length of the lens array, and g is the gap between the lens array and the EIA plane.

For each determined P'' point, EIAs are generated via the conventional II pickup method. An example of a generated EIA is illustrated in Fig. 3. Compared with conventional 360 degree IFD for the same object illustrated in Fig 3(a), the generated EIA is extended in the vertical direction due to the expandability of initial

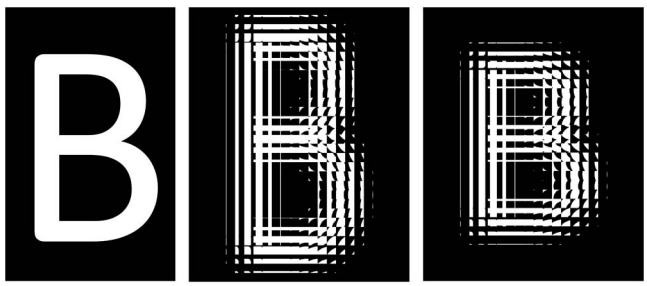

Fig. 3. (a) For the given character B, (b) the proposed method generates an EIA, which is extended in the vertical direction, compared with (c) an EIA generated by the conventional 360 degree IFD pickup process.

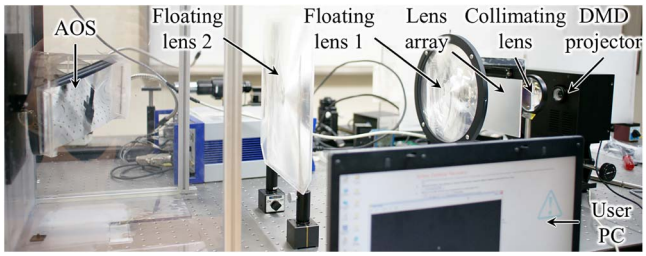

Fig. 4. Optical devices required in the real experiment on the optical table.

3D images, as shown in Fig. 3(b), where EIA size is similar to the object in the conventional case, as shown in Fig. 3(c).

The real experimental configuration is shown in Fig. 4. Note that our experimental setup of the entire system is laid down on the optical table for easier implementation. Specifications for the object and other optical devices are shown in Table 1.

EIAs are generated from the corresponding viewing directions around the 3D point cloud object "teapot and skeleton of cube." All of the object points of two point cloud objects have different depth information. The distance between the extreme fore point of the teapot and the extreme back point of the skeleton of the cube is 5 mm, as shown in Fig. 5(a). Objects from multiple viewing directions and corresponding generated EIAs are illustrated in Figs. 5(b) and 5(c), respectively. EIAs are aggregated 2D perspectives that are generated for each object point where there are 31866 object points, considering the azimuthal angle of the AOS and other optical devices, as explained previously. Also, the vertical size of initial 3D objects is expanded in the vertical direction as approximately 1.33 times, according to the shape and focal length of convex mirror in the EIA calculation process. The size of an EIA is 1024×768 pixels, the same as with the number of micromirrors of the DMD.

In the experiment, the DMD projector displays a total of 200 different EIAs per round in the generated order. The reconstructed initial 3D images via the lens array are relayed to the AOS while double floating lenses configured in the 4-f relay system and the motor rotates the convex mirror in synchronization with the projection.

Table 1. Specifications for the Objects and Optical Devices

Objects and Devices	Specifications
Initial point cloud 3D object (teapot & skeleton of cube)	Size = $35.69 \times 34 \times 40.33$ mm Total 31866 points
DMD projector	12 degree tilting XGA DMD
Collimating lens	Size = 100×100 mm $f_{CL} = 70$ mm
Lens array	Elemental lens pitch = 1 mm $f_{LA} = 3.3$ mm
Floating lens 1 (Fresnel lens)	Size = 170×170 mm $f_{FL1} = 110$ mm
Floating lens 2 (Fresnel lens)	Size = 280×280 mm $f_{FL2} = 318$ mm
AOS	Size = 150×100 mm $f_m = 87.65$ mm
Motor	SM3420 smart motor

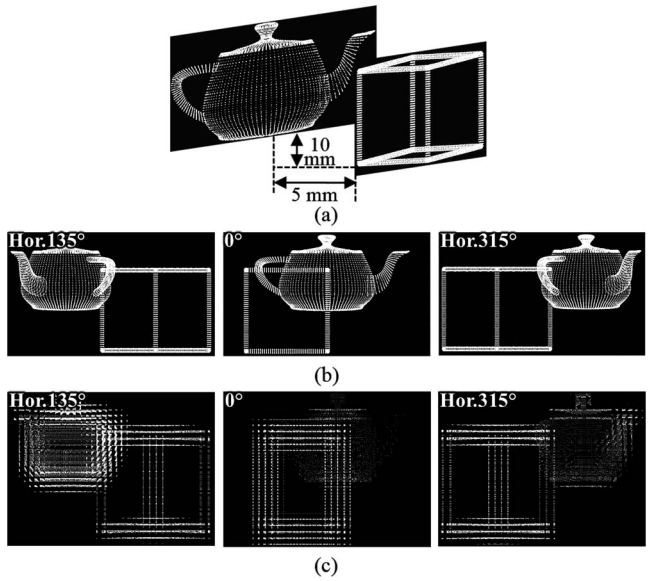

Fig. 5. (a) Two point cloud 3D objects with different information, (b) their representations from multiple viewing directions from 0, Hor.135 and Hor.315 degree around the object, and (c) the generated EIAs for the corresponding view perspectives.

Here, the viewing angle of initial 3D perspectives (~13 degree) is reduced to approximately 4 degree according to the double floating lenses function, to degrade the overlapping effect between angular projections on the AOS where the angular step of the AOS is 1.8 degree, same as a conventional 360 degree IFD system. Figure 6 shows the displayed 3D image on the rotating convex mirror from multiple viewing directions: from the front, the top, the bottom, and the sides. Total size of the displayed image in the AOS space is approximately 82×60 mm.

Viewing angle along the horizontal direction is 360 degree, so some example images to confirm a 360 degree viewing angle that captured images around the display (0, Hor.135 and Hor.315 degree each way) are presented in the middle line of Fig. 6. For the vertical direction, the viewing angle has been enhanced to approximately

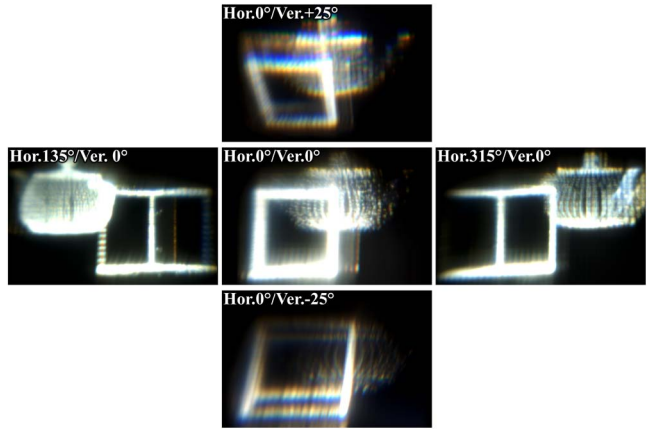

Fig. 6. Displayed image in the AOS space captured from nine viewing directions: the front (0 degree), some side views around the display horizontally (Hor.135 and Hor.315 degree), the top (Ver. + 25 degree) and bottom (Ver. – 25 degree) views along the vertical direction.

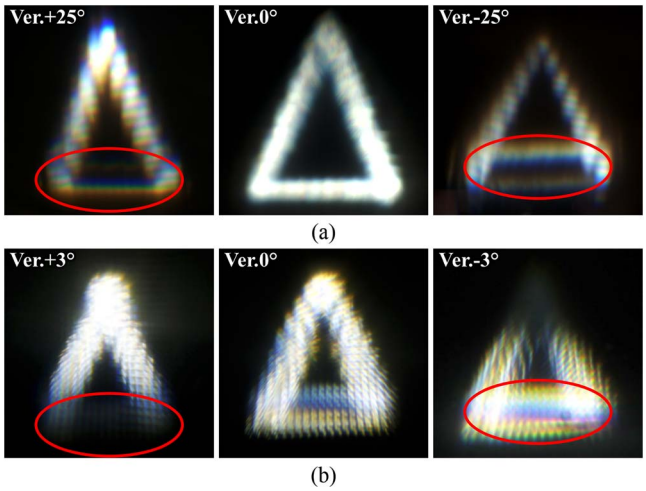

Fig. 7. Comparison for the VVA between (a) proposed and (b) conventional 360 degree IFD system when using the object "skeleton of a pyramid."

50 degree, where it was only about 4–6 degree in the conventional 360 degree IFD system [14].

Figure 7 shows the VVA comparison between proposed and conventional 360 degree IFD systems for the same 3D object "skeleton of a pyramid." Here, comparing the top and bottom views of displayed image in the AOS space, which is shown in Fig. 7(a), with the top and bottom view images of conventional system, shown in Fig. 7(b), VVA enhancement can be verified successfully.

In conclusion, we propose a VVA enhancing method for a conventional 360 degree IFD system using an AOS with a vertically curved convex mirror screen. The initially reconstructed 3D images via a lens array are relayed in different viewing directions in the AOS space horizontally, so 360 degree viewing zone is still achieved with the high angular light ray sampling. Unlike conventional 360 degree IFD, the AOS successfully improves VVA, as well (by approximately 50 degree), mainly because of the focal length of the rotating convex mirror. Also, double floating lenses increase the longitudinal and lateral depth ranges in the AOS space according to the double floating-lenses function, so a full-parallax depth-enhanced 360 degree 3D image with a wide VVA can be displayed with perfect depth cues of human visual perception. Further research will be focused on the elimination of the blurred reconstruction due to overlapped different angular 3D perspectives on the rotating mirror and resolution enhancement.

This work was supported by a National Research Foundation of Korea (NRF) grant funded by the Korea government (MSIP) (No. 2013-067321) and the Korea Creative Content Agency (KOCCA) in the Culture Technology (CT) Research & Development Program 2013.

References

1. G. Lippmann, C. R. Acad. Sci. **146**, 446 (1908).
2. J.-H. Park, K. Hong, and B. Lee, Appl. Opt. **48**, H77 (2009).
3. K.-C. Kwon, C. Park, M.-U. Erdenebat, J.-S. Jeong, J.-H. Choi, N. Kim, J.-H. Park, Y.-T. Lim, and K.-H. Yoo, Opt. Express **20**, 732 (2012).
4. G. Baasantseren, J.-H. Park, M.-U. Erdenebat, S.-W. Seo, and N. Kim, J. Soc. Inf. Disp. **18**, 519 (2010).
5. J. Kim, S.-W. Min, Y. Kim, and B. Lee, Appl. Opt. **47**, D80 (2008).
6. J.-S. Jang and B. Javidi, Appl. Opt. **42**, 1996 (2003).
7. S. Jung, J.-H. Park, H. Choi, and B. Lee, Opt. Express **11**, 1346 (2003).
8. Y. Kim, J.-H. Park, H. Choi, S. Jung, S.-W. Min, and B. Lee, Appl. Opt. **44**, 546 (2005).
9. R. Martinez-Cuenca, H. Navarro, G. Saavedra, B. Javidi, and M. Martinez-Corral, Opt. Express **15**, 16255 (2007).
10. H. Kim, J. Hahn, and B. Lee, Opt. Express **16**, 21865 (2008).
11. G. Baasantseren, J.-H. Park, K.-C. Kwon, and N. Kim, Opt. Express **17**, 14405 (2009).
12. M. A. Alam, M.-L. Piao, L. T. Bang, and N. Kim, Appl. Opt. **52**, 6969 (2013).
13. A. Jones, I. McDowall, H. Yamada, M. Bolas, and P. Debevec, Proc. ACM SIGGRAPH **26**, 1 (2007).
14. M.-U. Erdenebat, G. Baasantseren, N. Kim, K.-C. Kwon, J. Byeon, K.-H. Yoo, and J.-H. Park, J. Opt. Soc. Korea **16**, 365 (2012).
15. M.-U. Erdenebat, G. Baasantseren, J.-H. Park, N. Kim, K.-C. Kwon, Y.-H. Jang, and K.-H. Yoo, Proc. SPIE **7863**, 7863OU (2011).
16. D. Miyazaki, N. Akasaka, K. Okoda, Y. Maeda, and T. Mukai, Proc. SPIE **8288**, 82881H (2012).